

Drying of Solid Materials by Vacuum Fluidized Bed Dryer

Majid I. Abdul Wahab, Khalid. H. Rheima

Chemical Engineering Department - College of Engineering - University of Baghdad - Iraq

Abstract

In the present study the performance of drying process of different solid materials by batch fluidized bed drying under vacuum conditions was investigated. Three different solid materials, namely; ion exchange resin-8528, aspirin and paracetamol were used. The behavior of the drying curves as well as the rate of drying of these materials had been studied. The experiments were carried out in a 0.0381 m column diameter fluidized by hot air under vacuum conditions. Four variables affecting on the rate of drying were studied, these variables are vacuum pressure (100 - 500 mm Hg), air temperature (303-323 K), particle size (0.3-0.8 mm) and initial moisture content (0.35-0.55 g/g solid) for resin and (0.1-0.2 g/g solid) for aspirin and paracetamol. The study of the characteristics of the drying curves showed that the drying behavior depends mainly on the type of the solid material and on the operating conditions. It was found that the drying rate at vacuum conditions is enhanced by increasing the operating temperature of the air and decreases by increasing the initial moisture content of the material and the particle size. Moreover, an experiment was carried out to study the drying of aspirin solid material which is dried in atmospheric fluidized bed dryer operating at the same conditions to compare the temperature and time needed in both techniques. It was found that the temperature needed for vacuum fluidized bed dryer (303 K) is less than needed by fluidized bed dryer operating at atmospheric pressure (323 K). A simplified model for the drying of solids in the constant-rate period in a batch fluidized bed is developed, considering the bed to consist of dense phase and bubble phase with heat and mass transfer between the phases. It is assumed that the solids in dense phase to be in thermal equilibrium with the interstitial gas in the dense phase. The bubble size, its rise velocity, and the bubble volume fraction are taken into account while developing the model. The model is compared with experimental data reported in this study and found to match satisfactorily.

Introduction

Few researchers interested in fluidization at reduced pressure is due to the fact that low-pressure fluidized beds seemed not to be very interesting from the point of view of practical applications. However, this type of fluidization has a promising potential field in the fine chemicals solid as well as the pharmaceutical and food industry. Fine chemicals solid are often dried at the end of the manufacturing process, and as they are usually particulate materials, fluidized-bed drying seems to be a suitable procedure.

A problem arises from the fact that in a number of cases the moisture which must be removed by the

drying operation is constituted of an organic solvent.

Therefore, drying with hot air will easily lead to the formation of a mixture within the flammability limits; in these conditions, the risk of explosion is very high. This is the reason why fluidized-bed drying has been gradually put aside in many processes. Low-pressure fluidized-bed drying is therefore very interesting for such situations. ⁽¹⁾ Fluidized-bed features give optimum conditions for the treatment of granular materials, 0.the resulting atmosphere, giving the possibility of maintaining it outside the flammability conditions and ensuring a completely safe operation. Further-more, low-pressure fluidization leads to the use of much lower operating temperatures; this is a very important aspect if a thermo labile substance must be dried, as

the risk of degradation is much lower. [2]

The drying process, at relatively high temperatures or long residence times, may cause the partial degradation of thermolabile products. In addition, if, as is often the case in the pharmaceutical industry, the process is involved with evaporation of an organic solvent, a mixture within the flammability limits with a high risk of explosion can be formed. A fluidized bed operating under vacuum offers the possibility of eliminating these problems. Lower operating temperatures achieved under vacuum conditions reduce the probability of thermal degradation. At the same time, the low-pressure operation may provide a safer process out of flammability limits. [3]

Fluid-bed processes using organic solvent require an inert gas, such as nitrogen, to replace the air as the medium of fluidization and a solvent recovery system to condense out the solvent and recycle the gas. A vacuum fluid-bed system was presented by Luy et al.; a fluidized bed was generated and sustained under vacuum, thereby eliminating the use of inert gas. The developers claim several advantages for this system, such as considerable emission reduction, increased recovery rate of the solvent, and an application for oxygen-sensitive materials. [4]

The present work was aimed to study the characteristics of drying process in a batch fluidized bed dryer under reduced pressure (vacuum). The drying curves of three solid materials different in density were obtained and analyzed. Four variables are affecting the drying of these materials were investigated, namely; initial moisture content, particle size, air temperature and operating pressure. The aim also is to compare the characteristics of the vacuum fluidized bed drying process with the drying in the fluidized beds taking place at normal atmospheric pressure.

Experimental Work

The experiments in the present work were carried out to find the effects of some variables on the characteristics of drying of solids by fluidized bed dryer under vacuum conditions. The variables studied are: vacuum pressure, air temperature, initial moisture content and particle size. The range of variables selected was shown in Table 1. Three different materials were used, they are: aspirin, paracetamol, and ion exchange resin-8528, their properties are shown in Table 2.

Table 1 Range of Variables

Material	Pressure, mmHg	Air temperature, °C	Initial moisture content, g/solid	Particle size, mm
Aspirin	260,460,660	30,40, 50	0.1,0.15,0.2	-0.9+0.7 -0.7+0.5 -0.5+0.3
Paracetamol	460,560,660	30,40, 50	0.1,0.15,0.2	-0.9+0.5 -0.5+0.42 -0.42+0.18
Resin	400,500,600	30,35, 40	0.35,0.45,0.55	-0.9+0.7 -0.7+0.5 -0.5+0.1

Table 2 Properties of Materials Used

Property	Aspirin	Paracetamol	Resin
Bulk density, kg/m ³	787	583	607
Melting point, °C	135	169	120

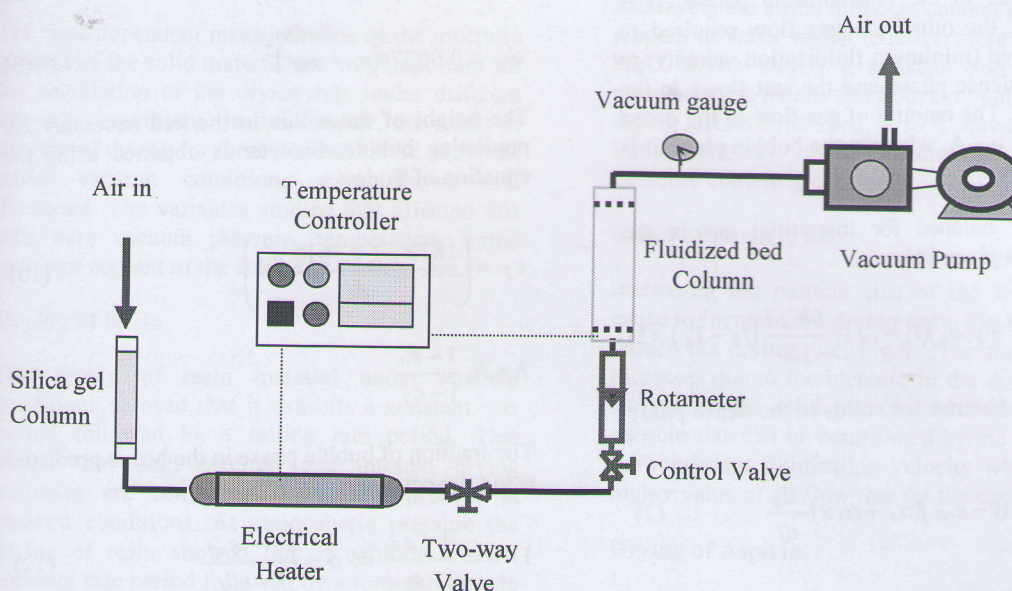


Figure 1 Schematic diagram of the experimental set-up

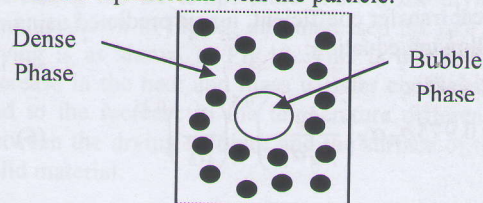
The experiment was begun by switching on the vacuum pump which allows the air to flow through the experimental unit at a certain flow rate adjusted by means of the rotameter. The power supply in the heating section was switched on to supply the heat from the heating element to the air. The temperature was adjusted at the desired temperature which was controlled by the temperature controller. When the desired temperature was reached as indicated by a thermometer placed directly after the heater, the air was allowed to pass to the column. Immediately, samples had been taken very quickly, especially at the beginning of the drying cycle to distinguish the warming up period, the time corresponding for each sample was recorded, then the sample placed in an oven controlled at a certain temperature. This was continued till the end of the process.

The samples had been taken from a hole at the bottom of the column opened and closed manually (as fast as possible), and each sample was placed in a weighted ceramic crucible and weighted to four decimal point by using a 4 digit balance (BL 210 s/type sartorius with max 210gm, $d=0.1$ mg). Then the sample was placed in an oven which temperature was controlled at 105°C for enough time until the material became bone dry. Each sample was taken out from the oven and placed into a desiccator, containing silica gel particles as the adsorbent media, until it was cooled then weighted and returned to the oven, this step was repeated for the same sample until a constant weight was reached. This procedure also repeated

for all the other samples. So, for each material, the moisture content variation versus time had been known, and then the rate of drying can be calculated.

Modeling

A simplified model for the drying of solids in the constant-rate period in a batch fluidized bed is developed in this study⁽⁵⁾. It assumes that the bed to be divided into two phases; dense phase and bubble phase with heat and mass transfer between the phases. Further, the model assumes that all the particles are homogeneous in character, spherical in shape and uniform in size during drying; all particles within the bed are at the same temperature and have the same moisture content at any time; and the drying medium leaving the fluidized bed is in thermal equilibrium with the particle.



Current knowledge of the drying kinetics in the constant-rate period suggests that resistance to drying is only from the gas phase surrounding the solids and that resistance of solids is negligible. The model assumes that gas in the dense phase is in equilibrium with the solids, attaining the wet-bulb temperature corresponding to the inlet gas temperature and humidity. The transfer rate

between the bubble and dense phases determines the drying rate in the constant-rate period. It is assumed that the minimum gas flow required to fluidize the bed (minimum fluidization velocity) to flows in the dense phase and the rest flows in the bubble phase. The amount of gas flow in the dense phase is $G_d = u_{mf} A$, while in the bubble phase it is $G_b = (u_i - u_{mf}) A$.

The enthalpy balance for interstitial gas in the dense phase is given by:

$$Q = \rho_g m_d (\alpha_g + y_i \alpha_v) (T_i - T_d) + \frac{6h_{bd}\delta}{d_b} (T_b - T_d) \quad (1)$$

The enthalpy balance for solids in the dense phase is given by:

$$Q = \lambda R'_c + \rho_s (1 - \epsilon_{mf}) (\alpha_s + \alpha_v x) \frac{dT_s}{dt} \quad (2)$$

Substituting equation (1) in to (2), the amount of moisture removed from the bed is:

$$R'_c = \frac{\rho_g m_d (\alpha_g + y_i \alpha_v) (T_i - T_d) + \frac{6h_{bd}\delta}{d_b} (T_b - T_d) - \rho_s (1 - \epsilon_{mf}) (\alpha_s + \alpha_v x) \left(\frac{dT_s}{dt} \right)}{\lambda} \quad (3)$$

The enthalpy balance for the bubble phase is written as:

$$\rho_g m_b (\alpha_g - y_i \alpha_v) (T_i - T_b) = \frac{6h_{bd}\delta}{d_b} (T_b - T_d) \quad (4)$$

On rearranging equation (4), the bubble temperature, T_b , becomes:

$$T_b = \frac{\rho_g m_b (\alpha_g + y_i \alpha_v) T_i d_b + 6h_{bd} T_d \delta}{6h_{bd} \delta + \rho_g m_b (\alpha_g - y_i \alpha_v) d_b} \quad (5)$$

The heat transfer coefficient, h_{bd} , is predicted using the following equation:

$$h_{bd} = 0.975 \rho_g \alpha_g \left(\frac{k_g}{\rho_g \alpha_g} \right)^{0.5} \left(\frac{g}{d_b} \right)^{0.25} \quad (6)$$

The bubble diameter is predicted using the following equation:

$$d_b = d_{bm} - (d_{bm} - d_{bo}) e^{-0.3H/D} \quad (7)$$

$$d_{bm} = 0.652 [A_c (u_i - u_{mf})]^{0.4} \quad (8)$$

$$d_{bo} = 0.00376 (u_i - u_{mf})^2 \quad (9)$$

The height of the solids in the bed necessary for predicting bubble diameter is obtained using the equation of Todes:

$$\epsilon_f = \left(\frac{18 Re_p + 0.36 Re_p^2}{Ar} \right)^{0.2} \quad (10)$$

$$h = h_o \frac{1 - \epsilon_o}{1 - \epsilon_f} \quad (11)$$

The fraction of bubble phase in the bed is predicted using the equation:

$$1 - \delta = \frac{1 - \epsilon_f}{1 - \epsilon_{mf}} \Rightarrow \delta = \frac{\epsilon_f - \epsilon_{mf}}{1 - \epsilon_{mf}} \quad (12)$$

The minimum fluidization velocity is predicted using the equation:

$$u_{mf} = \frac{\mu}{d_p \rho_g} \left[\left[(33.7)^2 + 0.0408 Ar \right]^{0.5} - 33.7 \right] \quad (13)$$

The drying rate in constant-rate period can be estimated solving equation (3), which requires, the dense phase temperature, T_d , the bubble phase temperature, T_b , the bubble diameter, d_b , the heat transfer coefficient between bubble phase and dense phase, h_{bd} and the volume fraction of bubbles in the bed, δ . The dense phase temperature, T_d , is assumed to be in wet bulb temperature corresponding to the inlet air temperature and humidity where as the bubble phase temperature, T_b , is estimated using equation (5). The heat transfer coefficient between the bubble and dense phase is estimated using equation (6) and the bubble diameter, d_b , is estimated using equation (7). The volume fraction of bubbles, δ , in the bed is estimated using equation (12).

The third term in the numerator of equation (3) corresponds to the rate of sensible heat rise of the material in the dense phase. Under steady state operation, in constant-rate drying period the temperature of the material in the dense phase essentially remains constant and hence the term is insignificant.

Results and Discussion

The time dependent measurements of the moisture content of the solid material are very important for the calculation of the drying rate under different operating conditions. In this chapter, the result of the rate of drying for three different solid materials under vacuum conditions were shown and discussed. The variables studied that affected this rate were vacuum pressure, temperature, initial moisture content of the solid and particle size.

Drying of Resin

The drying of resin material under vacuum conditions showed that it exhibits a constant rate period followed by a falling rate period. This means that both external and internal drying variables are controlled the drying process at vacuum conditions. At atmospheric pressure the drying of resin showed that it exhibits a short constant rate period followed by a long falling rate period which means that the internal variables are controlled. The vacuum conditions moved the drying process to be controlled by both external and internal drying variables. This agrees the results of Arnaldos who observed that the effect of reducing the operating pressure is greater on drying rates of porous particles.

Effect of Operating Pressure

Increasing the vacuum pressure decreasing the drying time to reach the same moisture content as shown in Fig.2. Also the rate of drying is increased and still has a constant and falling rate periods as shown in Fig.2. The rate of drying is increased due to the increase in the internal diffusivity through the porous structure of the solid particle and the increase in the mass transfer coefficient. This agrees with Kozanoglu (2001) who indicated that at vacuum operating conditions the diffusion coefficient of gas is increased and that Sherwood number takes higher values

Effect of Air Temperature

An increase in Air temperature decreasing the drying time and as a result increasing the drying rate as shown in Fig.4 and 5. The magnitude of the constant rate period increases due to the increase in the heat and mass transfer coefficients and to the increase in the temperature difference between the drying medium and the wet surface of the solid material.

Effect of initial moisture content

An increase in initial moisture content cause to increase time for drying and as a result decreasing

the rate of drying as shown in Fig.6 and 7. Increasing the initial moisture content increased the amount of water which required more drying time. Fig.7 shows clearly a constant and falling rate periods which means that both external and internal drying factors controlled. Also it showed that as the initial moisture content decreased, the critical moisture content decreased.

Effect of Particle size

Increasing the particle size of the solid material cause to increase the drying time, Fig.8 and also to reduce the drying rate, Fig.9. The time of drying increases due to the increase in the distance to the surface of the solid particle. Also increasing the particle size can be contributed by the increases of the minimum fluidization velocity which needs a higher value of air flow rate for the same duty.

Drying of Aspirin

The fluidized bed drying of aspirin under vacuum conditions showed that it exhibits a long constant rate period. This means that the over all heat and mass transfer (the rate of drying) is controlled by external drying factors. In this case, the operating pressure and temperature are of importance in the drying of aspirin while the initial moisture content and particle size became of decreasing importance. The behavior of the characteristics drying curves of aspirin under vacuum conditions shoed that it is of the hygroscopic non-porous materials.

Effect of Operating Pressure

Decreasing the operating pressure caused to decrease the drying time and to increase the rate of drying (Fig.10, 11). This is due to the increase in the mass transfer coefficient under vacuum conditions.

Effect of Air Temperature

Increasing the air temperature shorten the drying time as shown in Fig.12, and increased the rate of drying is as shown in Fig.13. This is due to the increase in the heat and mass transfer coefficients and to the increase in the temperature difference between the drying medium and the surface of the solid material.

Effect of Initial moisture content

An increase in the initial moisture content need more drying time (Fig.14) and the rate of drying is slowly decreased (Fig.15). The initial moisture content has no significant effect on the rate of drying of aspirin as shown in Fig.15. This means that internal factors have no significant effect

(external factors control).

Effect of Particle size

As the particle size increased the drying time increased and the rate of drying is decreased (Fig.16, 17). It can be say that the drying rate is not affected significantly by the particle diameter and the constant rate period is around the same order of magnitude.

Drying of Paracetamol

The drying of paracetamol showed that it exhibits a long constant rate period and short falling rate period which means that external drying factors are controlled. This behavior of drying rate curves means that the material is of hygroscopic non-porous type, and evaporation takes place only at the surface of the solid material and all liquid is physically bond and the moisture moves by diffusion.

Figures 18- 25 show the effects of various operating conditions on the moisture content-time and the rate of drying-moisture content. Generally,

Table 3 Comparison between atmospheric and vacuum fluidized bed drying of aspirin

Operating conditions	Atmospheric fluidized bed dryer ⁽⁶⁾	Vacuum fluidized bed dryer*
Air temperature, °C	50	30
Initial moisture content, %	15	15
Final moisture content, %	0.5	0.5
Drying time, min.	57	40

* Operating pressure=260 mm Hg.

It is shown that although the Air temperature is much less in the case of vacuum fluidized bed drying, the drying time is shorter in this case which indicate that the vacuum drying process is more efficient and economical.

Solution of the Process Model

The model is simulated to assess the effects of various operating parameters on the drying kinetics and the following observations are made. An increase in gas rate or its temperature increases the

the effects are the same as for other types of solid materials discussed above.

Decreasing the operating pressure caused to decrease the drying time, Fig.18 and increases the rate of drying, Fig.19. Increasing the air temperature, enhances the moisture content decrease with time of drying, Fig.20, and increases the rate of drying, Fig.21. For example the moisture content change from 20% to 1% during 58 minute at 30 °C, while it takes 33 minute at 50 °C. Increasing the initial moisture content increased the drying time, since the amount of water is increased, Fig.22, this is due to that all the moisture is physically bound. The results showed that the initial moisture content has no significant effect on the rate of drying, Fig.23. The effect of particle size of the solid is that the time of drying increased and the rate of drying decreased by increasing the particle size, Fig.24, Fig.25.

Comparison between Atmospheric and Vacuum Fluidized Bed Drying

A comparison between atmospheric and vacuum fluidized bed drying of aspirin was achieved depending on the air temperature and drying time for the same duty.

drying rate while an increase in the inlet gas humidity or the bubble volume fraction decreases the drying rate. An increase in the solids hold-up decreases the drying rate due to decrease in the input enthalpy per unit mass of solids. The simulations are performed by varying one parameter at a time keeping the other parameters constant. However in practice an increase in air rate increases the bubble volume fraction as well as bed height. The simulation results qualitatively agree with earlier predictions reported in literature. The model is compared with experimental data in this study. Figure 26 shows a comparison of the experimental data with the prediction using the model. It can be observed that the experimental data compare satisfactorily with the model.

Nomenclature

- A area of the bed, m²
- D diameter of the bed, m
- d diameter, m
- G flow rate, m³/s
- g gravitational constant
- H height of the fluidized bed, m
- h heat transfer coefficient, J/m² s °C
- k thermal conductivity, J/m s °C
- m gas flow rate per unit volume of the bed, s⁻¹
- P pressure, mm Hg
- ΔP pressure drop, N/m²

- Q total heat input per unit volume of the bed, $J/m^3 s$
 R rate of drying, $g/g \text{ solid} \cdot \text{min}$
 R' rate of moisture removal per unit volume of bed, $kg/m^3 s$
 T temperature, $^{\circ}C$
 t time, minute
 u gas velocity in the bed, m/s
 W solid hold-up, kg
 w moisture content, $g \text{ moisture} / g \text{ solid}$
 y gas humidity, $g \text{ moisture} / g \text{ dry air}$

Subscripts

- b bubble
 bd bubble to dense phase
 c critical, constant
 d dense phase
 e equilibrium
 f fluidized bed
 g gas
 i inlet
 mf minimum fluidization
 o static
 p particle
 s solid
 v vapour

Greek letters

- ρ density, kg/m^3
 α specific heat, $J/kg \text{ } ^{\circ}C$
 λ latent heat of evaporation, J/kg
 ϵ void fraction
 μ viscosity of the gas, $kg/m s$
 δ volume fraction of bubbles in the bed

Dimensionless groups

- Ar Archimedes number, $d_p^3 g \rho_g (\rho_s - \rho_g) / \mu^2$
 Re_p Reynolds number, $\rho_d u / \mu$

References

1. Leuenberger, H., Luy, B. and Hirschfeld, P., "Esperimenti con un nuovo sistema a letto fluido sottovuoto", *Tecnol. Chim.*, 11, 100-105, 1991.
2. Llop, M.F., Madrid, F., Arnaldos, J., and Casal, J., "Fluidization at vacuum conditions: a generalized equation for the prediction of minimum fluidization velocity", *Chem. Eng. Sci.* 51, 5149, 1996.
3. Kozanoglu, B. U., Vilchez, J. A., Casalb, J. and Arnaldos, J., "Mass transfer coefficient in vacuum fluidized bed drying", *Chemical Engineering Science* 56, 3899-3901, 2001
4. Luy, B., Hirschfeld, P. and Leuenberger, H., "Granulation and Drying in Vacuum Fluidized-Bed Systems", *Pharm. Ind.* 51, 89 (1989).
5. Srinivasakannan, C. and Balasubramanian, N., "A Simplified Approach to the Drying of Solids in a Batch Fluidized Bed", *Brazilian Journal of Chemical Engineering*, Vol. 19, No.03, pp. 293-298, July-September 2002.
6. Al-Hussaini, M.M., "Drying of Solid Materials by Fluidized Beds", M.Sc. Thes. 2004.

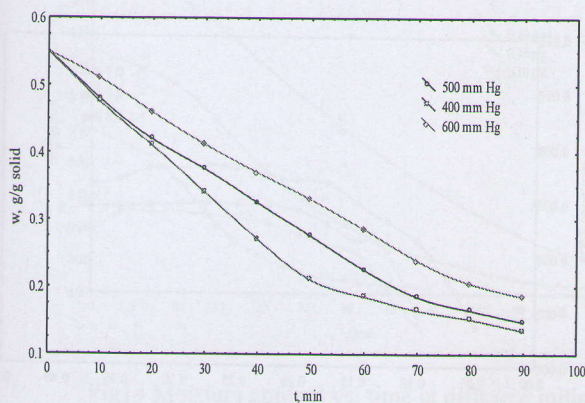


Fig.2 Moisture content vs. time at different operating pressure ($w=0.55 \text{ g/g}$, $T=30 \text{ } ^{\circ}C$, $d=0.3 \text{ mm}$)

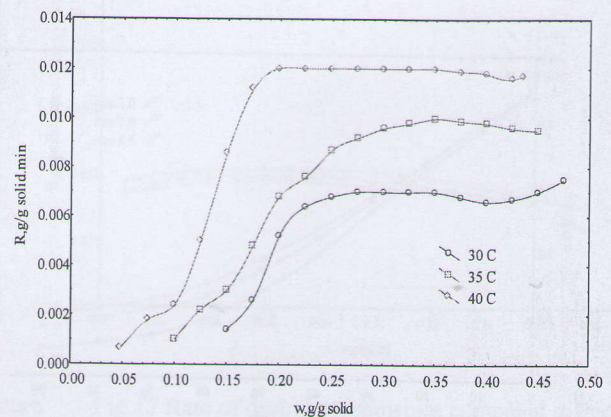


Fig.5 Rate of drying vs. moisture content at different temperatures ($w=0.55 \text{ g/g}$, $P=400 \text{ mm Hg}$, $d=0.3 \text{ mm}$)

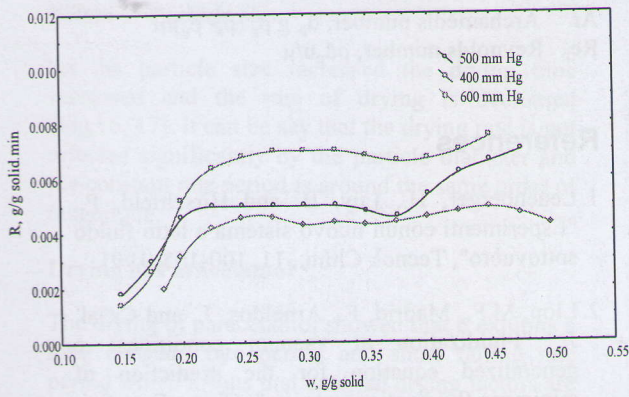


Fig 3 Rate of drying vs. moisture content at different operating pressure ($w=0.55$ g/g, $T=30$ °C, $d=0.3$ mm)

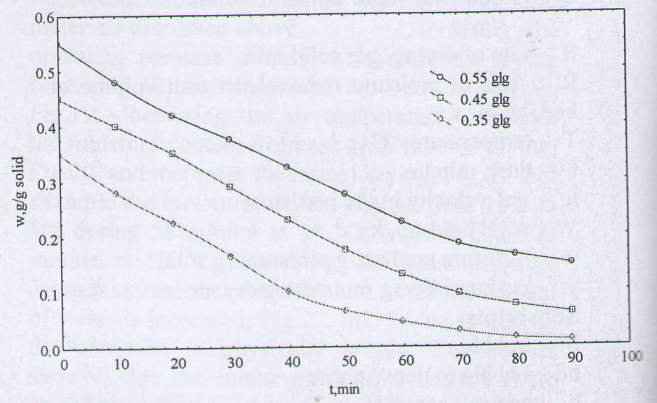


Fig.6 Moisture content vs. time at different initial moisture contents ($P=500$ mm Hg, $T=30$ °C, $d=0.3$ mm)

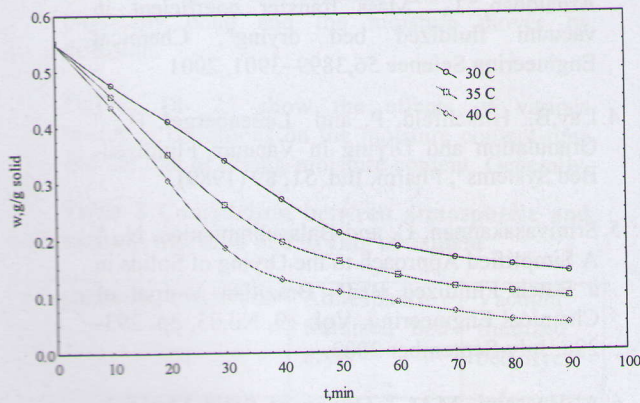


Fig.4 Moisture content vs. time at different temperatures ($w=0.55$ g/g, $P=400$ mm Hg, $d=0.3$ mm)

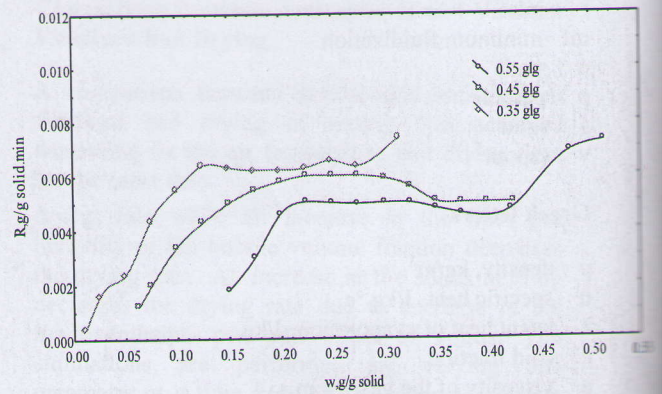


Fig.7 Rate of drying vs. moisture content at different initial moisture content ($P=500$ mm Hg, $T=30$ °C, $d=0.3$ mm)

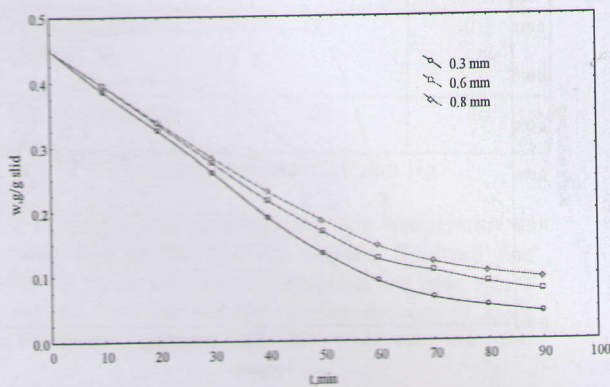


Fig.8 Moisture content vs. time at different particle size ($P=400$ mmHg, $T=30$ °C, $w=0.45$ g/g)

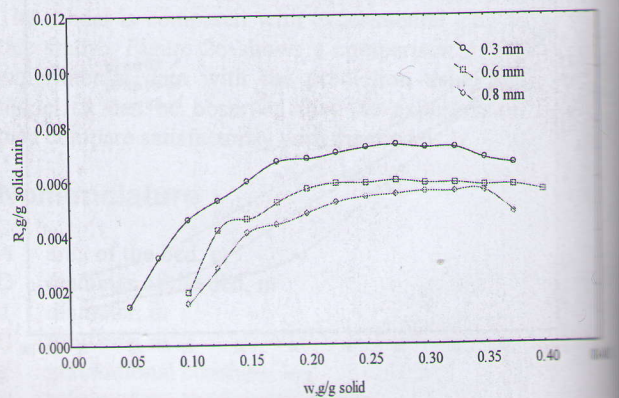


Fig.11 Rate of drying vs. moisture content at different operating pressure ($w=0.2$ g/g, $T=30$ °C, $d=0.4$ mm)

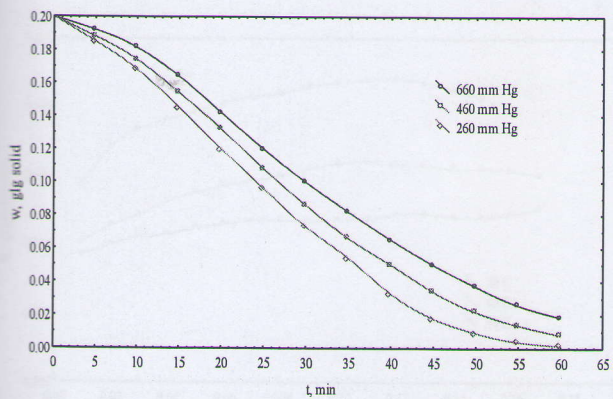


Fig.9 Rate of drying vs. moisture content at different particle size (P=400mmHg, T=30 °C, w=0.45 g/g)

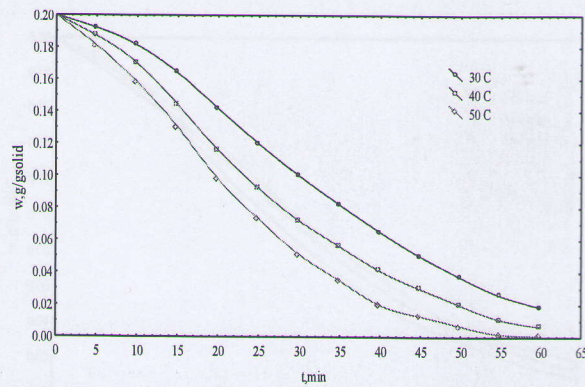


Fig.12 Moisture content vs. time at different drying temperature (w=0.2g/g, P= 660 mm Hg, d=0.4 mm)

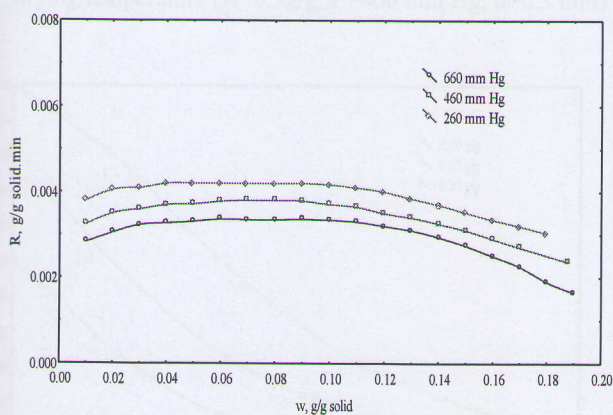


Fig.10 Moisture content vs. time at different operating pressure (w=0.2g/g, T=30 °C, d=0.4 mm)

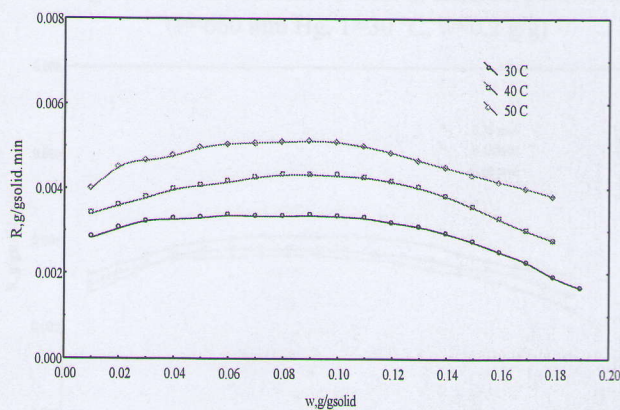


Fig.13 Rate of drying vs. moisture content at different drying temperature (w=0.2g/g, P= 660 mm Hg, d=0.4 mm)

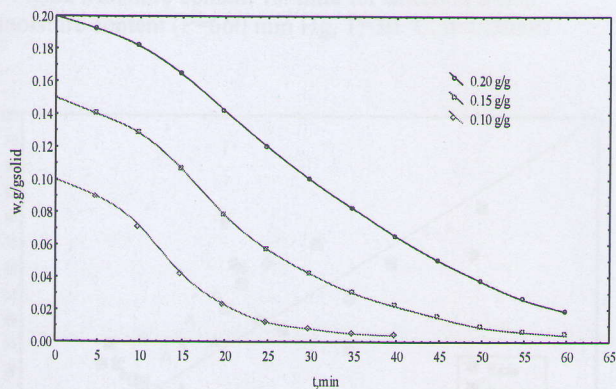


Fig.14 Moisture content vs. time at different initial moisture content (P= 660 mm Hg, T=30 °C, d=0.4 mm)

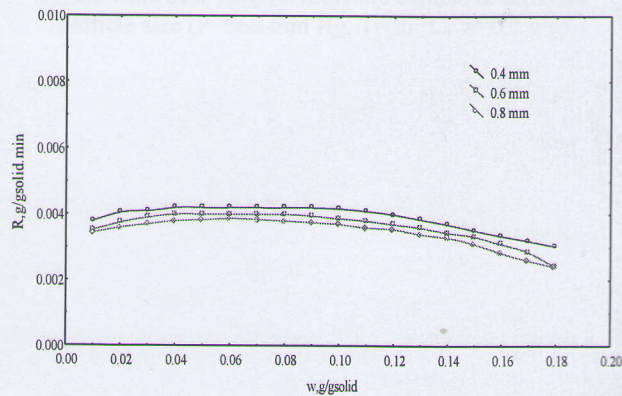


Fig.17 Rate of drying vs. moisture content at different particle size (w=0.2 g/g, P=260 mm Hg, T=30 °C)

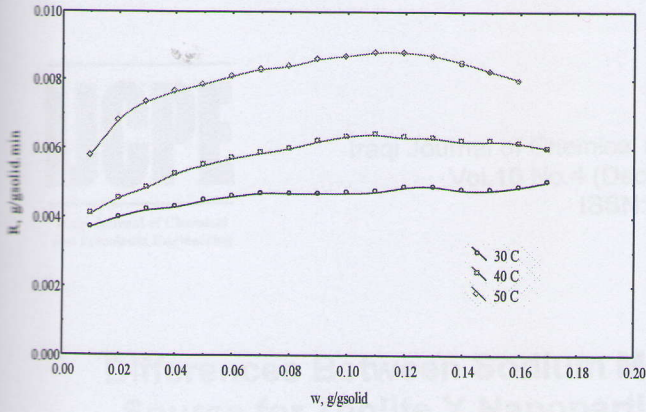


Fig.21 Rate of drying vs. moisture content at different drying temperature ($w=0.2g/g$, $P=460$ mm Hg, $d=0.3$ mm)

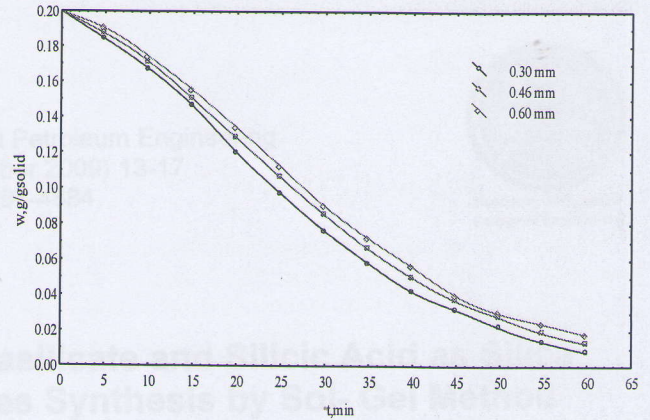


Fig.24 Moisture content vs. time at different particle size ($P=660$ mm Hg, $T=30$ °C, $w=0.2$ g/g)

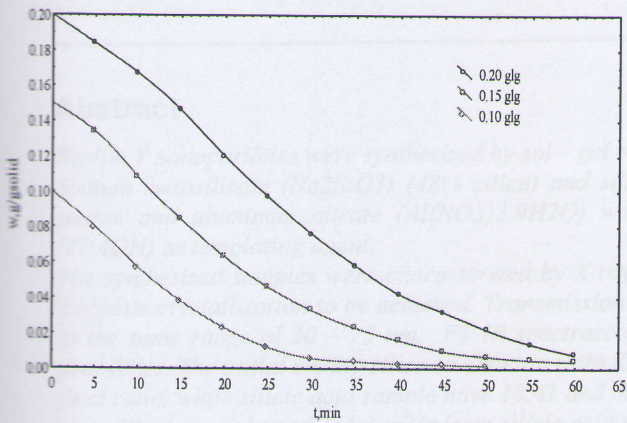


Fig.22 Moisture content vs. time for different initial moisture content ($P=660$ mm Hg, $T=30$ °C, $d=0.3$ mm)

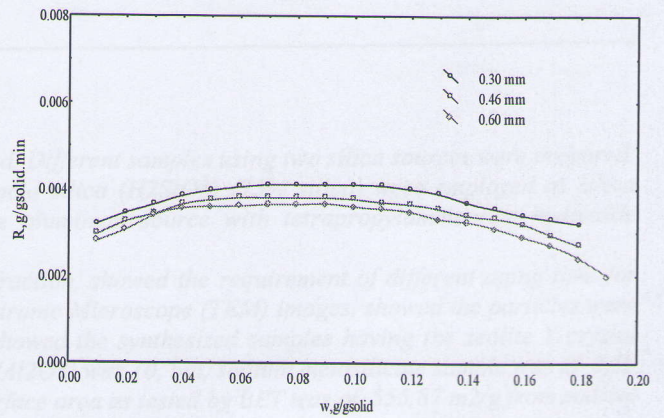


Fig.25 Rate of drying vs. moisture content at different particle size ($P=660$ mm Hg, $T=30$ °C, $w=0.2$ g/g)

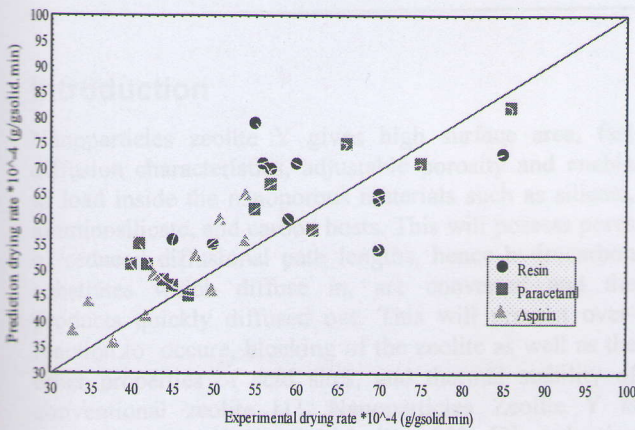


Fig.26 Comparison of experimental drying rate with the predicted value